J. DONG ✉
A. SHIRAKAWA
K.-I. UEDA

Sub-nanosecond passively Q-switched Yb:YAG/Cr^{4+}:YAG sandwiched microchip laser

Institute for Laser Science, University of Electro-Communications, 1-5-1 Chofugaoka, Chofu, Tokyo 182-8585, Japan

ABSTRACT We report on laser-diode pumped low-threshold, and compact passively Q-switched Yb:YAG microchip lasers, with Cr^{4+}:YAG crystals as the saturable absorbers. The laser threshold at the fundamental wavelength of 1.03 μm is as low as 0.25 W, and the slope efficiency is as high as 36.8%, and the optical-to-optical efficiency is as high as 27% for the 95% initial transmission of the Cr^{4+}:YAG crystal. A pulse width of 1.35 ns and peak power of over 8.2 kW was obtained. Using a 5 mm thick KTP crystal as the second-harmonic generation medium, 514.7 nm green light of 155 mW power was generated. The pulse duration of 480 ps was generated at 1.03 μm by using 85% of the initial transmission of the Cr^{4+}:YAG saturable absorber. Stable single-longitudinal-mode oscillation and wide-separated multi-longitudinal-mode oscillation due to the etalon effect of the Cr^{4+}:YAG thin plate was achieved at different pump power levels.

PACS 42.55.Sa; 42.55.Xi; 42.60.Gd

1 Introduction

Passively Q-switched solid-state lasers with high peak powers have potential use in optical communications, pollution monitoring, nonlinear optics, material processing and medical surgery, nonlinear frequency conversion and so on. Passively Q-switched solid-state lasers are usually achieved by using neodymium-doped crystals as the gain media and Cr^{4+}:YAG [1] or semiconductor saturable absorber mirror (SESAM) [2] as the saturable absorber. Recently, high power laser-diode pumped Yb:YAG lasers have been demonstrated [3]. Compared with Nd:YAG laser material, Yb:YAG crystal has several advantages such as a long storage lifetime (951 μs) [4], a very low quantum defect (8.6% with a pump wavelength of 941 nm and a laser wavelength of 1030 nm), resulting in three times less heat generation during lasing than comparable Nd-based laser

systems [5]. Other advantages include a broad absorption bandwidth and less sensitivity to diode wavelength specifications [6], a relatively large emission cross section [7] suitable for Q-switching operation, and easy growth of high quality and moderate concentration crystal without concentration quenching [8].

Another reason for interest in Yb:YAG lasers is that the frequency doubled wavelength of 515 nm matches the highest power line of Ar-ion lasers, thereby leading to the possibility of an all solid-state replacement [9]. Compared with SESAM, Cr^{4+} doped bulk crystals as the saturable absorber has several advantages, such as a high damage threshold, low cost, and simplicity. A passively Q-switched Yb:YAG laser with Cr^{4+}:YAG as the saturable absorber was first demonstrated by using a Ti:sapphire laser as the pump source [10]. Passively Q-switched Yb:YAG microchip lasers with 530 ps pulse widths have been obtained by

using SESAM [11]. Recently, a laser-diode pumped Cr,Yb:YAG microchip laser with a pulse width of 440 ps, and a peak power of over 53 kW has been demonstrated [12], however, owing to co-doping of chromium ions with Yb into the YAG host, the fluorescence lifetime decreases [13] with an increase of Cr concentration, and there is strong absorption (about 60% of that around 1 μm) of the pump power by Cr^{4+} at the pump wavelength (around 940 nm) owing to the broad absorption spectrum of Cr^{4+}:YAG from 800 nm to 1300 nm [14, 15]. The absorbed pump power threshold is high due to the high intracavity loss induced by the defects occurring on introducing Cr ions into the Yb:YAG crystal for compact Cr,Yb:YAG microchip lasers. The passively Q-switched microchip laser configuration of a sandwiched saturable absorber between gain medium and output coupler, proposed by Zayhowski et al. about two decades ago [1], should be an alternative way to overcome the pump power absorption loss of Cr^{4+}, and to achieve highly efficient laser operation with short pulse widths in passively Q-switched Yb:YAG/Cr^{4+}:YAG microchip lasers. A short resonator cavity length will permit short pulse operation, separation of the gain medium and the saturable absorber will eliminate defects introduced into the Cr,Yb:YAG crystal. The Cr^{4+}:YAG crystal only acts as a saturable absorber, and is not an additional loss to the pump power as occurs in Cr,Yb:YAG crystals.

Frequency doubling of a Q-switched laser is a convenient method to construct compact, pulsed sources in the blue-green region. These devices are of interest in communications, displays, chemical processing, and as pump sources

✉ Fax: +81-0424-85-8960, E-mail: dong@ils.uec.ac.jp

for laser materials. Frequency doubling could be realized by either placing appropriate nonlinear crystals inside or outside the resonator. Intracavity frequency doubling is a well-developed way to convert the fundamental wavelength to green or blue in continuous-wave (cw) operation or Q-switched laser operation with different active media, various saturable absorbers, as well as different frequency doubling nonlinear crystals [16–19]. Besides the complicated cavity design of intracavity frequency doubling, long pulse generation will be a disadvantage for intracavity frequency doubling of passively Q-switched lasers owing to the long cavity, caused by placing a frequency doubling crystal inside the laser cavity. The extracavity frequency doubling has the advantages of simple laser cavity design, by just placing the frequency doubling crystal near the output coupler of the passively Q-switched solid-state lasers. Because of the high peak power generated in the passively Q-switched Yb:YAG microchip lasers with Cr^{4+}:YAG as the saturable absorber, extracavity frequency doubling will be a better choice than intracavity frequency doubling. Efficient extracavity frequency doubling generation from ultraviolet to the visible range has been reported by using passively Q-switched Nd:YAG microchip lasers [1, 20–22].

In this paper, we report the experimental investigations of laser-diode end-pumped low-threshold, compact passively Q-switched Yb:YAG/Cr^{4+}:YAG microchip lasers by using different initial transmissions (T_0) of Cr^{4+}:YAG saturable absorbers. The extracavity frequency doubling of passively Q-switched Yb:YAG/Cr^{4+}:YAG lasers was also investigated. 155 mW green light at 514.7 nm was generated by using this passively Q-switched Yb:YAG/Cr^{4+}:YAG microchip laser with

$T_0 = 95\%$ Cr^{4+}:YAG saturable absorber. The differences between passively Q-switched Yb:YAG/Cr^{4+}:YAG microchip lasers and monolithic Cr,Yb:YAG microchip lasers [12] were addressed by the same pump power level. Owing to the broad emission spectrum of Yb:YAG crystal and the etalon effect of the Cr^{4+}:YAG thin plate inside the cavity, the laser was operated at wide-separated multi-longitudinal-modes at a high pump power range. Stable single-longitudinal-mode oscillation can be obtained at a low pump power range. The widely separated multi-longitudinal-mode oscillation at high pump power ranges was addressed based on the asymmetrical broad emission spectrum of the Yb:YAG crystal and the etalon effect of the Cr^{4+}:YAG thin plate sandwiched between the Yb:YAG crystal and the output coupler.

2 Experimental setup

The configuration of laser-diode end-pumped sandwiched passively Q-switched Yb:YAG microchip lasers with Cr^{4+}:YAG crystals as saturable absorbers was very simple and compact. The stability of such sandwiched microchip resonators was supported by the pump-induced thermal lens, thermal expansion and gain guiding effects. The short cavity length (1.5 mm) and flexibility of varying the initial transmission of the saturable absorber, in order to change the modulation depth of the saturable absorber, allowed for short pulse oscillations below 1 ns during Q-switched laser operation. Figure 1 shows a schematic diagram of the experimental setup for a passively Q-switched Yb:YAG microchip laser with a Cr^{4+}:YAG as the saturable absorber. Yb:YAG crystal and Cr^{4+}:YAG crystals were grown by the traditional Czochralski method. A plane-parallel,

1 mm thick Yb:YAG crystal was doped with 10 at. % Yb as the gain medium. One surface of the crystal was coated for anti-reflection at 940 nm and total reflection at 1.03 μm thus acting as one cavity mirror. The other surface was coated for high transmission at 1.03 μm and total reflection at 940 nm to increase the absorption efficiency of the pump power. An additional advantage of this coating is the fact that the pump beam does not pass the Cr^{4+}:YAG saturable absorber, and therefore does not influence the performance of the Q-switched regime (Cr^{4+}:YAG also presents absorption at 940 nm). Three 0.5 mm thick Cr^{4+}:YAG crystals with different initial transmissions ($T_0 = 95, 90$ and 85%), which acted as Q-switches, were sandwiched between a Yb:YAG sample and a plane-parallel output coupler with 20% transmission. The saturated transmissions of these three Cr^{4+}:YAG crystals are 99, 97.5 and 96% for $T_0 = 95$, 90 and 85%, respectively. The choice of 20% transmission of the output coupler is based on the Q-switched laser theory [23, 24], the higher the transmission of the output coupler, the higher the pulse energy. The high transmission of the output coupler will also reduce the intracavity laser intensity to avoid coating damage. Total cavity length was 1.5 mm. A high-power fiber-coupled 940 nm laser diode with a core diameter of 100 μm and numerical aperture of 0.22 was used as the pump source. Two lenses of 8 mm focal length were used to focus the pump beam on the crystals rear surface and to produce a pump light footprint in the crystal of about 100 μm in diameter. About 95% of the pump power is incident on the Yb:YAG crystal after passing through the coupling optics. The laser was operated at room temperature. A 5 mm thick KTP crystal was used as a nonlinear conversion crystal. The KTP crystal was angle cut for type II phase matching of 1030 nm ($\theta = 90°$, $\varphi = 49.9°$), and was polished to be plane-parallel. Both surfaces of the KTP crystal were coated with antireflection coatings at both the fundamental wavelength ($R < 0.2\%$) and the second-harmonic wavelength ($R < 0.5\%$). The Q-switched pulse profiles were recorded by using a fiber-coupled InGaAs photodiode with a bandwidth of 16 GHz (the rise time from 10% to 90% is 25 ps), and a 7 GHz Tektronix
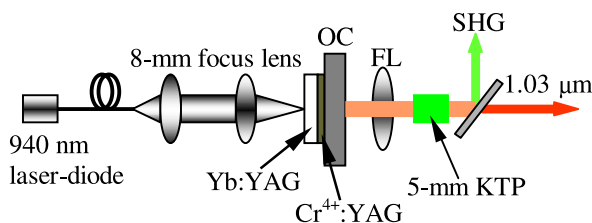

FIGURE 1   A schematic diagram of a laser-diode pumped passively Q-switched Yb:YAG microchip laser using a Cr^{4+}:YAG crystal as the saturable absorber. OC, output coupler; SHG, second harmonic generation; FL, focus lens with 100 mm focal length

TDS7704B digital phosphor oscilloscope. The laser spectrum was analyzed by using an optical spectrum analyzer. The laser output beam profile was monitored using a CCD camera both in the near-field and the far-field of the output coupler.

3   Results and discussion

Continuous-wave (cw) operation of a 1 mm Yb:YAG microchip laser was performed ahead of the passively Q-switched laser experiments. The laser operates in a TEM$_{00}$ mode with multiple (two to six) longitudinal modes. The absorbed pump power threshold was 240 mW, and the slope efficiency was over 58%. An output power of 1.15 W was obtained when the absorbed pump power was 2.5 W, and the corresponding optical-to-optical efficiency was 46%. Passively Q-switched Yb:YAG/Cr^{4+}:YAG microchip laser performance was studied first by using a $T_0 = 95\%$ Cr^{4+}:YAG crystal as the saturable absorber. The pump power threshold is about 0.25 W, and the average output power as a function of absorbed pump power was shown in Fig. 2. Average output power increases linearly with the absorbed pump power, and the average output power increases slowly with the absorbed pump power when the absorbed pump power is lower than 1 W the slope efficiency is about 17.7%, while the slope efficiency is about 36.8% when the absorbed pump power is higher than 1 W. The change of the slope efficiency is attributed to an increase of the laser mode area and the pump power intensity at high pump power. There was no pump saturation, therefore, the output power can be scaled with a high pump power. A maximum average output power of 676 mW was obtained when the absorbed pump power was 2.5 W, corresponding to an optical-to-optical efficiency of 27%. The repetition rate increases linearly from 980 Hz at an absorbed pump power of 0.25 W to 63 kHz at an absorbed pump power of 2.5 W. The pulse width (FWHM) decreases very slowly from 2.3 ns at an absorbed pump power of 0.25 W to 1.35 ns at an absorbed pump power of 2.5 W. The pulse energy increases very slowly with the absorbed pump power, from 3 µJ at an absorbed pump power of 0.25 W to 10.8 µJ at an absorbed pump power of 2.5 W. The peak power of the passively Q-switched Yb:YAG microchip laser increases from 1.1 kW at an absorbed pump power of 0.25 W to 8 kW at an absorbed pump power of 2.5 W. The output laser transverse intensity profile was close to TEM$_{00}$ and was near-diffraction-limited with an M^2 of less than 1.1. Although the maximum average output power of 23 mW with a pulse width of 2.1 ns at a repetition rate of 5.5 kHz was obtained at an absorbed pump power of 0.33 W for stable single-longitudinal-mode oscillation, it should be noted that stable single-longitudinal-mode oscillation could be obtained by increasing the pump beam diameter incident on the laser crystal at higher pump powers. Extracavity frequency doubling was performed by focusing the output fundamental pulsed laser, at 1030 nm, to the KTP crystal using a focussing lens with 100 mm focal length. The beam diameter of the fundamental laser incident on the KTP crystal was measured to be 80 µm, which is the same as the beam diameter near the output coupler. The average output power of the second harmonic generation (SHG) also increases linearly with absorbed pump power. The highest average output power of 155 mW at 514.7 nm was achieved, as shown in Fig. 2. High efficient SHG should be achieved by optimizing the length of the KTP crystal and the beam diameter of the fundamental laser. There is no observation of the pulse width variation for the incident fundamental laser pulses and the green pulses. This may be due to the low fundamental laser intensity. 2.5 µJ green pulses with pulse duration of 1.35 ns were obtained at an absorbed pump power of 2.5 W.

By using low initial transmissions of Cr^{4+}:YAG crystals, Q-switched laser pulses with short pulse width and high peak power were obtained. An average output power of 190 mW was achieved by using a $T_0 = 90\%$ Cr^{4+}:YAG crystal when the absorbed pump power was 1.35 W. There was coating damage occurrence with further increase of the pump power. The coating damage was caused by the high intracavity intensity and low damage threshold of the coating, which can be avoided by improving the coating quality. A pulse energy of 11 µJ with pulse width of 578 ps at a repetition rate of 17.2 kHz was achieved by using a $T_0 = 90\%$ Cr^{4+}:YAG saturable absorber when the absorbed pump power of 1.35 W was used without coating damage. The resulting peak power was over 19 kW. The pulse width of 480 ps was obtained by using a $T_0 = 85\%$ Cr^{4+}:YAG saturable absorber with the absorbed pump power of 1.2 W without coating damage, which is shorter than those obtained by using SESAM as the saturable absorber for a passively Q-switched Yb:YAG microchip laser [11]. In addition, the Q-switched laser pulses with a pulse energy of 13 µJ and a peak power over 27 kW, at a repetition rate of 9.2 kHz, shows that this passively Q-switched Yb:YAG/ Cr^{4+}:YAG microchip laser, as a potential compact source for generating laser pulses with high pulse energy and high peak power, as compared to a passively Q-switched Yb:YAG microchip laser with SESAM as the saturable absorber. Figure 3 shows the
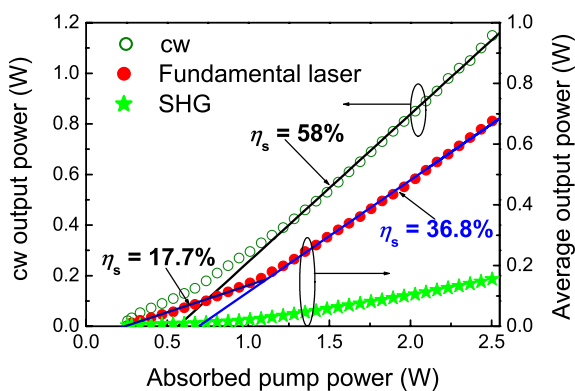

FIGURE 2   Output power of a 1mm thick Yb:YAG microchip laser, and the average output power of the fundamental laser and second-harmonic-generation as a function of the absorbed pump power, for a passively Q-switched Yb:YAG microchip laser with a $T_0 = 95\%$ Cr^{4+}:YAG crystal as the saturable absorber
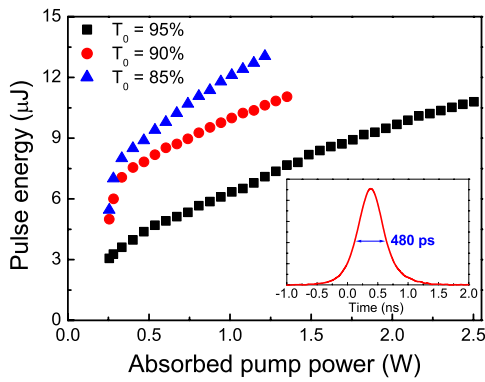
comparison of the output pulse energy for three different initial transmissions of the Cr^{4+}:YAG crystals as a function of the absorbed pump power. The oscilloscope trace of the output pulse with a pulse width of 480 ps and a pulse energy of 13 μJ for a $T_0 = 85\%$ Cr^{4+}:YAG saturable absorber is also shown in the inset of Fig. 3. The pulse energy increases with a decrease of the initial transmission of the Cr^{4+}:YAG saturable absorber under the same pump power level and transmission of the output coupler. The pulse energy should be further increased by increasing the pump power if the coating damage problem can be solved. As the absorption cross section of the Cr^{4+}:YAG is much larger than the emission cross section of the Yb:YAG crystal, the resulting pulse width can be estimated as follows [1, 10],

$$t_p = \frac{0.86t_r}{\gamma_{\text{sat.r}}} \left[\frac{\delta\,(1+\delta)\,\eta}{\delta - \ln(1+\delta)} \right], \qquad (1)$$

where t_r is the cavity round-trip time, η is the energy extraction efficiency of the laser pulse given by the implicit relationship $\eta\,(1+\delta) = -\ln(1-\eta)$, and $\delta = \gamma_{\text{sat,r}}/(\gamma_{\text{par,r}} + \gamma_{\text{op}})$ is the ratio of saturable loss, $\gamma_{\text{sat,r}}$, to unsaturable cavity loss, $\gamma_{\text{par,r}}$ is the round-trip unsaturable intracavity parasitic loss, and γ_{op} is the output coupling loss. By putting these experimental data values $\gamma_{\text{op}} = 0.223$, $\gamma_{\text{par,r}} = 0.128, 0.165$, and 0.198, $\gamma_{\text{sat,r}} = 0.105, 0.223$ and 0.357 for $T_0 = 95$, 90 and 85%, respectively, into (1), the pulse widths of this kind of passively Q-switched Yb:YAG microchip lasers were estimated to be 650 ps, 330 ps and 220 ps for $T_0 = 95$, 90 and 85%, respectively, which are in fair agreement with the experimental pulse widths. The discrepancy between measured pulse widths and expected pulse widths is at-

tributed to the thermal effects within the active medium, and some uncertainties in the determination of unsaturable parasitic intracavity loss and saturable loss.

The optical-to-optical efficiency of passively Q-switched Yb:YAG/Cr^{4+}: YAG microchip lasers decreases with a decrease of the initial transmission of the Cr^{4+}:YAG saturable absorber, however, the absorbed pump power threshold (0.25, 0.26 , and 0.27 W for $T_0 = 95$, 90 and 85%, respectively) is lower than that for the Cr,Yb:YAG microchip self-Q-switched laser (680 mW) under the same pump conditions. The lower absorbed pump power thresholds of passively Q-switched Yb:YAG/Cr^{4+}:YAG microchip lasers indicate the lower intracavity loss for passively Q-switched Yb:YAG/Cr^{4+}:YAG microchip lasers, than that for the Cr,Yb:YAG microchip laser even though there is optical loss introduced by the mechanical contacts among the gain medium, saturable absorber, and the output coupler. However, the pulse width of 578 ps by using a 90% initial transmission is longer than the pulse width of 440 ps obtained in the Cr,Yb:YAG microchip laser [12]. The pulse energy of 11 μJ and peak power of 19 kW is lower than that obtained in the Cr,Yb:YAG microchip laser under the same pump condition (i.e. at an absorbed pump power of 1.35 W). The pulse width discrepancy between these two lasers with 90% initial transmission of the Cr^{4+}:YAG was attributed to the difference of the laser cavity length (1.5 mm for Yb:YAG/Cr^{4+}:YAG laser, 1 mm for Cr,Yb:YAG microchip laser). The higher repetition rate of Yb:YAG/Cr^{4+}: YAG microchip laser (17.2 kHz) on comparing to the Cr,Yb:YAG microchip laser (5 kHz) under the same pump conditions, (e.g. at absorbed pump power

of 1.35 W) was caused by a higher pump rate (the ratio of absorbed pump power to absorbed pump power threshold) of 5.2 for the Yb:YAG/Cr^{4+}:YAG microchip laser than that of 2.0 for the Cr,Yb:YAG microchip laser. The pulse energy difference between the two lasers was attributed to the difference of the initial inversion populations; the higher the initial inversion population, the higher the output pulse energy as indicated in [23]. The initial inversion population is proportional to the intracavity loss of passively Q-switched lasers for the same initial transmission of the saturable absorber and output coupling. The higher absorbed pump power threshold for the Cr,Yb:YAG microchip laser means a higher intracavity loss even with 15% transmission of the output coupler. Therefore, the high pulse energy was obtained in the Cr,Yb:YAG microchip laser at lower pump rates when comparing the low pulse energy at high pump rates for the Yb:YAG/Cr^{4+}:YAG sandwiched microchip lasers. The low intracavity loss of the Yb:YAG/Cr^{4+}:YAG sandwiched microchip lasers can be fully used to obtain a high pulse energy output by a decrease of the initial transmission of the Cr^{4+}:YAG saturable absorber. The output pulse energy of the passively Q-switched Yb:YAG microchip lasers with Cr^{4+}:YAG as the saturable absorber can be improved by using optical bonding technology or composite ceramic technology [25], to further reduce the optical loss introduced by the mechanical contacts, and by using the low initial transmission of the Cr^{4+}:YAG saturable absorber to increase the initial inversion population.

Laser spectra indicated that this passively Q-switched Yb:YAG/Cr^{4+}:YAG microchip laser can oscillate in single-longitudinal-mode oscillation and multi-longitudinal-mode oscillation depending on the pump power level. Figure 4 shows the laser spectra of passively Q-switched Yb:YAG microchip lasers with a $T_0 = 95\%$ Cr^{4+}:YAG as the saturable absorber. Single-longitudinal-mode oscillation at 1029.4 nm was obtained when the absorbed pump power was kept below 0.3 W. Multi-longitudinal-mode oscillation dominated at high pump power regimes. The separation between each mode was measured to be 0.58 nm, which is three times wider
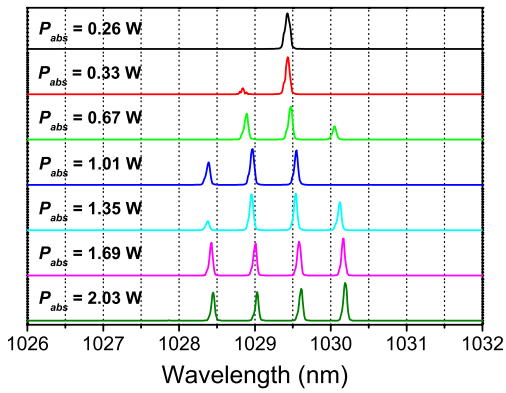
FIGURE 4   Laser spectra of a passively Q-switched Yb:YAG with $T_0 = 95\%$ Cr^{4+}:YAG as the saturable absorber at different absorbed pump powers. The resolution of the optical spectral analyzer is 0.05 nm

than the separation between the longitudinal modes (0.194 nm) in the laser cavity filled with the gain medium predicted by [26] $\Delta\lambda_c = \lambda^2/2L_c$, where L_c is the optical length of the resonator, and λ is the laser wavelength. The cause of the wide separation between each mode is attributed to the Cr^{4+}:YAG thin plate which acts as an intracavity tilted etalon to select longitudinal modes [26]. Figure 5 shows the output longitudinal modes selected by the Cr^{4+}:YAG thin plate etalon in the passively Q-switched Yb:YAG/Cr^{4+}:YAG microchip laser. Owing to the broad emission spectrum of the Yb:YAG around 1.03 μm, many longitudinal modes can be excited even for a 1 mm thick Yb:YAG crystal. Microchip cw Yb:YAG lasers operate in a multi-longitudinal-mode over the whole pump power region [27]. Figure 5a shows the gain profile of the Yb:YAG crystal and the resonant modes determined by the cavity length. Figure 5b shows the transmission of the etalon as a function of wavelength with different reflectivity of the Cr^{4+}:YAG etalon, the difference between two adjacent maximum transmissions of the etalon is given by $\Delta\lambda = \lambda^2/2nd$, where d is the thickness of the Cr^{4+}:YAG.

The peak transmission of the etalon strongly depends on the reflectivity of the etalon, the higher the reflectivity, the narrower the transmission bandwidth. The desired oscillating resonant modes can be selected by using a high reflectivity Cr^{4+}:YAG etalon or a high concentration, thin Cr^{4+}:YAG plate. For a 0.5 mm thick Cr^{4+}:YAG thin plate, because the ratio of cavity length to the thickness of Cr^{4+}:YAG thin plate is an integer, the resonant modes coinciding with the peak transmission of the Cr^{4+}:YAG thin plate will oscillate and other resonant modes will be suppressed to oscillate, therefore, the separation between the output laser modes is determined by the free spectral range of the Cr^{4+}:YAG etalon to be 0.58 nm (Fig. 5c). Of course, the possible oscillating laser modes are governed by the gain profile (Fig. 5a) and the nonlinear mode coupling effect between the possible output modes. Stable single-longitudinal-mode oscillation can be achieved by using a thinner Cr^{4+}:YAG plate with a high Cr^{4+} concentration at a high pump power range, based on the above observed results and theoretical predictions. The linewidth of each mode was less than 0.05 nm, limited

by the resolution of the optical spectra analyzer. The central wavelength of 1029.4 nm shifts to a longer wavelength, which is caused by the temperature dependent emission spectrum of the Yb:YAG crystal [7]. The relative intensity of each mode changes with pump power, which has effect on the fluctuation of the output pulse trains. The fluctuation of the output pulse trains is also caused by the cross-saturation mechanism, due to the strong spatial hole burning effect in the Yb:YAG to couple the longitudinal modes via population gratings and nonlinear absorption of the Cr^{4+}:YAG saturable absorber [28].

4   Conclusions

In conclusion, passively Q-switched Yb:YAG microchip lasers with different Cr^{4+}:YAG crystals as the saturable absorbers, have been investigated by adopting a sandwiched configuration for the first time. Slope efficiency of 36.8% and optical-to-optical efficiency of 27% at the fundamental wavelength of 1.03 μm have been obtained by using 95% of the initial transmission of the Cr^{4+}:YAG saturable absorber. 155 mW green light has been generated by this microchip passively Q-switched Yb:YAG/Cr^{4+}:YAG laser. Laser pulses with 480 ps pulse duration and 13 μJ pulse energy at 1.03 μm have been demonstrated by using 85% of the initial transmission of the Cr^{4+}:YAG saturable absorber, whereby a peak power of over 27 kW was obtained. There is a trade-off between the efficiency, pulse width, pulse energy and the threshold. The best compromise among them can be chosen depending on the applications of the laser. The lower intracavity loss of passively Q-switched Yb:YAG/Cr^{4+}:YAG sandwiched microchip lasers can be fully exploited to achieve a high output pulse energy by decreasing the initial transmission of the Cr^{4+}:YAG saturable absorber. Cr^{4+}:YAG thin plate also acts as an etalon for selecting longitudinal modes. Single-longitudinal mode, and wide-separated ($\Delta\lambda = 0.58$ nm) multi-longitudinal mode oscillation were obtained, depending on the pump power level. Stable single-longitudinal-mode oscillation could be obtained by choosing a thinner Cr^{4+}:YAG plate with a high Cr^{4+} concentration in passively Q-switched Yb:YAG/Cr^{4+}:YAG mi-
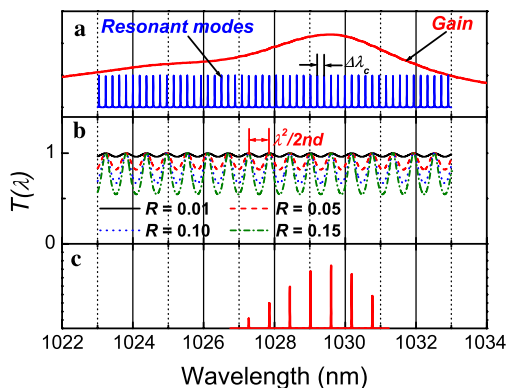

FIGURE 5   Laser mode selection mechanism of a passively Q-switched Yb:YAG/Cr^{4+}:YAG microchip laser with Cr^{4+}:YAG as an intracavity etalon. (**a**) Gain profile of the Yb:YAG crystal and resonant modes determined by the cavity length. (**b**) Transmission of Cr^{4+}:YAG thin plate as a function of laser wavelength with different reflectivities of the Cr^{4+}:YAG thin plate. (**c**) Possible output laser spectra selected by Cr^{4+}:YAG etalon

crochip lasers, and by increasing the pump beam diameter at high pump powers.

REFERENCES

1 J.J. Zayhowski, C. Dill III, Opt. Lett. **19**, 1427 (1994)
2 B. Braun, F.X. Kartner, G. Zhang, M. Moser, U. Keller, Opt. Lett. **22**, 381 (1997)
3 C. Stewen, K. Contag, M. Larionov, A. Giessen, H. Hugel, IEEE J. Sel. Top. Quantum Electron. **6**, 650 (2000)
4 D.S. Sumida, T.Y. Fan, Opt. Lett. **19**, 1343 (1994)
5 T.Y. Fan, IEEE J. Quantum Electron. **QE-29**, 1457 (1993)
6 H.W. Bruesselbach, D.S. Sumida, R.A. Reeder, R.W. Byren, IEEE J. Sel. Top. Quantum Electron. **3**, 105 (1997)

7 J. Dong, M. Bass, Y. Mao, P. Deng, F. Gan, J. Opt. Soc. Am. B **20**, 1975 (2003)
8 F.D. Patel, E.C. Honea, J. Speth, S.A. Payne, R. Hutcheson, R. Equall, IEEE J. Quantum Electron. **QE-37**, 135 (2001)
9 T.Y. Fan, J. Ochoa, IEEE Photon. Technol. Lett. **7**, 1137 (1995)
10 J. Dong, P. Deng, Y. Liu, Y. Zhang, J. Xu, W. Chen, X. Xie, Appl. Opt. **40**, 4303 (2001)
11 G.J. Spuhler, R. Paschotta, M.P. Kullberg, M. Graf, M. Moser, E. Mix, G. Huber, C. Harder, U. Keller, Appl. Phys. B **72**, 285 (2001)
12 J. Dong, A. Shirakawa, S. Huang, Y. Feng, T. Takaichi, M. Musha, K. Ueda, A.A. Kaminskii, Laser Phys. Lett. **2**, 387 (2005)
13 J. Dong, P. Deng, J. Luminesc. **104**, 151 (2003)
14 H. Eilers, U. Hommerich, S.M. Jacobsen, W.M. Yen, K.R. Hoffman, W. Jia, Phys. Rev. B **49**, 15 505 (1994)
15 R. Feldman, Y. Shimony, Z. Burshtein, Opt. Mater. **24**, 333 (2003)
16 V.G. Ostroumov, F. Heine, S. Kuck, G. Huber, V.A. Mikhailov, I.A. Shcherbakov, Appl. Phys. B **64**, (1997)

17 T.T. Kajava, A.L. Gaeta, Opt. Commun. **137**, 93 (1997)
18 Y.F. Chen, IEEE Photon. Technol. Lett. **9**, 1481 (1997)
19 N. Pavel, J. Saikawa, T. Taira, Opt. Commun. **195**, 233 (2001)
20 T. Taira, Y. Matsuoka, H. Sakai, A. Sone, H. Kan, in *CLEO/QELS Conf. 2006* (CA, USA, 2006), p. CWF6
21 J.J. Zayhowski, IEEE Photon. Technol. Lett. **9**, 925 (1997)
22 J.J. Zayhowski, Opt. Mater. **11**, 255 (1999)
23 J.J. Degnan, IEEE J. Quantum Electron. **QE-31**, 1890 (1995)
24 J.J. Degnan, IEEE J. Quantum Electron. **QE-25**, 214 (1989)
25 H. Yagi, T. Yanagitani, H. Yoshida, M. Nakatsuka, K. Ueda, Japan. J. Appl. Phys. **45**, 133 (2006)
26 W. Kochner, *Solid State Laser Engineering* (Springer, Berlin, 1999)
27 J. Dong, A. Shirakawa, K. Ueda, J. Xu, P. Deng, Appl. Phys. Lett. **88**, 161 115 (2006)
28 J. Dong, K. Ueda, Appl. Phys. Lett. **87**, 151 102 (2005)